

High Voltage gain Transformer less Fly back Converter

J V Pavan Chand*, N Sriharish*, Ch Rambabu*, V Sravan Kumar**

* Department of Electrical and Electronics Engineering, Sri Vasavi Engineering College.

** Department of Electrical and Electronics Engineering, Lakireddy Bali Reddy College of Engineering

Abstract

Conventional boost converters are unable to provide high step-up voltage gains due to the effect of power switches, rectifier diodes, and the equivalent series resistance of inductors and capacitors. This paper proposes high voltage gain transformer less Boost Converter without an extremely high duty ratio. Some dc-dc converters can provide high step-up voltage gain, but with the penalty of either an extreme duty ratio or a large amount of circulating energy. In the proposed converters, two inductors with the same level of inductance are charged in parallel during the switch-on period and are discharged in series during the switch-off period. The structures of the proposed converters are very simple. Only one power stage is used. High-efficiency, high step-up dc-dc converters with simple topologies are proposed in this paper.

1. Introduction

Fossil fuels are hydrocarbons, primarily coal, fuel oil or natural gas, formed from the remains of dead plants and animals. These are non-renewable resources because they take millions of years to form, and reserves are being depleted much faster than new ones are being made. The production and use of fossil fuels raise environmental concerns. A global movement toward the generation of renewable energy is therefore under way to help meet increased energy needs.

Electricity production: (i) Hydroelectricity continue to be a major resource. However, installations in main important sites are suffering from three factors: modest local consumption, the need to protect natural sites, and the shortage of financial capabilities. Still, small water heads are increasingly being exploited, especially in China, and Wind generators are being commercially distributed, either to supply electricity in long networks or to satisfy the needs for specific local applications. Some thermal power plants that burn organic residues are operational. Diverse types of solar thermal power plants are the subject of research; prototypes are being constructed and, in some cases, are already operational. Stand-alone photovoltaic systems are commercially marketed for rural electrification in developing countries. These supply electricity to isolated houses and have various professional applications. Grid-connected

Photovoltaic systems are the subject of numerous demonstrations, either in the form of central stations or integrated to building façades and roofs. Research on photovoltaic lanterns indicates a considerable level of technical progress.

A boost converter with a high voltage gain is used for many applications, such as lamp ballasts for automobile headlamps, fuel-cell energy conversion systems, solar-cell energy conversion systems, and battery backup systems for uninterruptible power supplies. Theoretically high voltage gain can be achieved by with high duty ratio [1]–[3]. Due to the effect of power switches, rectifier diodes, and the equivalent series resistance (ESR) of energy storage elements the voltage gain is reduced. Moreover Reverse recovery problem occurs with an operation of extremely high duty ratio [4]–[24]. A dc-dc fly back converter is a very simple structure with a high step-up voltage gain and an Electrical isolation, but the active switch of this converter will have a high voltage stress due to the presence of leakage inductance of the transformer. By having less voltage stress on the active switch and recycling the energy of leakage inductance, some energy - regeneration techniques have been used to reduce the voltage stress on the active switch and to recycle the leakage – inductance energy [4]–[6]. Technique using coupled- inductor will provide a solutions to have a low voltage stress on the active switch, high voltage gain, and having high efficiency without using high duty ratio [7]–[15].

Literature includes some research of the transformer less dc-dc converters, which includes quadratic boost type [17], cascade boost type[16], the capacitor-diode voltage multiplier type [21]–[22], the voltage-lift type [18]–[20], and the boost integrating with switched capacitor technique, the disadvantage is this complex and higher cost.

The switched inductor technique is used in three converters, in which two inductors with same level of inductance are charged in parallel during the switch-on period and are discharged in series during switch off period, to achieve high step up voltage gain with low duty ratio. Some conditions are assumed to analyze the steady state characteristics and operating principles i.e., all capacitors are sufficiently large, constant voltage across the capacitance, the voltage drop of diodes and on state resistance of the active switches is

ideal, and ESRs are ignored in inductors and capacitors.

2. FLYBACK CONVERTER SYSTEM

A. Basic Converter

The modified boost type with switched-inductor technique is shown in Fig: 1 [24]. The structure of this converter is very simple, In this we have only one power stage is used in this converter we have only one power stage is used in this converter.

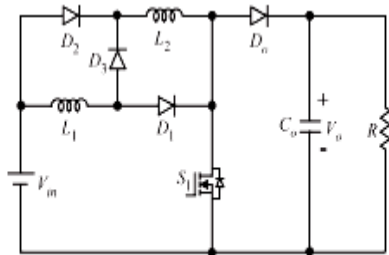


Fig:1

However, this converter has two issues: 1) Three power devices exist in the current-flow path during the switch-on period, and two power devices exist in the current flow path during the switch-off period; and 2) the voltage stress on the active switch is equal to the output voltage. For getting higher step-up voltage gain, the other dc-dc converters are also presented

B. Converter - I

The Converter I has the following merits compared with basic converter : 1) Two power devices exist in the current-flow path during the switch-on period, and one power device exists in the current flow path during the switch-off period; 2) the voltage stresses on the active switches are less than the output voltage; and 3) under the same operating conditions, including input voltage, output voltage, and output power, the current stress on the active Switch during the switch-on period is equal to the half of the current stress on the active switch of the converter in basic converter. This converter utilize the switched inductor technique, in which two inductors with same level of inductance are charged in parallel during the switch-on period and are discharged in series during the switch-off period to achieve high step-up voltage gain without the extremely high duty ratio.

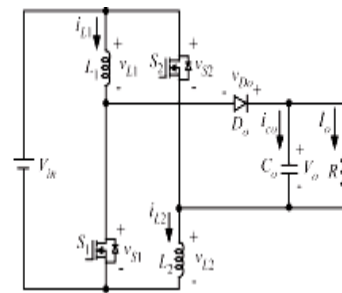


Fig:2

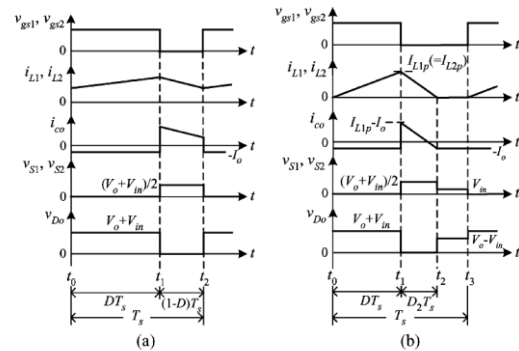


Fig: 3

This converter is shown in Fig: 2 It has two active switches S1 and S2, two inductors having same value of inductance L1 and L2, one output D0, and one output capacitor C0. Switches are controlled simultaneously by using single control signal. During continuous conduction mode (CCM) and discontinuous conduction mode (DCM) the typical waveform are obtained as shown in Fig 3. The operating principles and steady state analysis of CCM and DCM are presented in detail as follows.

I. CCM Operation

The operating modes can be divided into two modes, defined as modes 1 and 2.

1. **Mode 1**[t₀, t₁]. During this time interval, switches S₁ and S₂ are turned on.

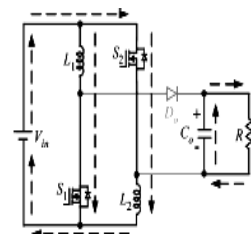


Fig:4(a)

The equivalent circuit is shown in Fig: 4(a). Inductors L₁ and L₂ are charged in parallel from the dc source, and the energy stored in the output capacitor C₀ is released to the load. Thus, the voltages across L₁and L₂ are given as

$$V_{L1}=V_{L2}=V_{in} \quad (1)$$

2. **Mode 2** [t₁,t₂]. During this time interval, S1 and S2 are turned off. The equivalent circuit is shown in Fig: 4(b).

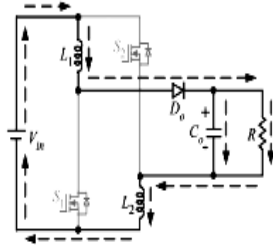


Fig: 4 (b)

The dc source, L₁, and L₂ are series connected to transfer the energies to C₀ and the load. Thus, the voltages across L₁ and L₂ are derived as

$$V_{L1}=V_{L2}=(V_{in}-V_o)/2 \quad (2)$$

By using the volt-second balance principle on L₁ and L₂, the following equation can be obtained:

$$\int_0^{DT_s} V_{in} dt + \int_{DT_s}^{Ts} (V_{in}-V_o)/2 \quad (3)$$

By Simplifying (3) the voltage gain is

$$M_{CCM} = \frac{V_{in}}{V_o} = \frac{1+D}{1-D} \quad (4)$$

The voltage stresses on S₁, S₂, and D₀ are derived as

$$V_{S1}=V_{S2}=(V_{D0})/2 \text{ Where } V_{D0}=V_{in}+V_o \quad (5)$$

II. DCM Operation

The operating modes for the proposed converter –I is divided into three modes

1. **Mode 1** [t₀,t₁]. The operating principle is same as that modes 1 in CCM operation and the peak current of L₁ and L₂ are

$$I_{L1p}= I_{L2p} =V_{in}DT_s/L \quad (6)$$

Where L=L₁=L₂

2. **Mode 2** [t₁, t₂]: During this time interval, S₁ and S₂ are turned off. The equivalent circuit is shown in Fig. 6(b). The dc source, L1 and L2 are series connected to transfer the energies to C₀ and the load. Inductor currents i_{L1} and i_{L2} are decreased to zero at t=t₂. Another expression of I_{L1p} and I_{L2p} is given as

$$I_{L1p}= I_{L2p} = \frac{V_o-V_{in}}{2L} D_2 T_s \quad (7)$$

3. **Mode 3** [t₂, t₃]: During this interval the both switches S₁ and S₂ are still turned off. The equivalent circuit is shown in Fig. 4(c).

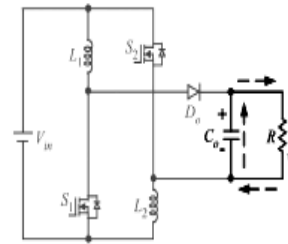


Fig: 4 (c)

The energies stored in L₁ and L₂ is zero. Thus only energy stored in C₀ is discharged to the load. From (6) and (7)

$$D_2 = 2DV_{in}/(V_o - V_{in}) \quad (8)$$

From Fig. 4(b), the average value of the output-capacitor current during each switching period is given by

$$I_{C0} = \frac{1}{2} D_2 I_{L1p} - I_o \quad (9)$$

$$I_{C0} = D^2 V_{in}^2 T_s / L (V_o - V_{in}) - V_o / R \quad (10)$$

Then the normalized inductor time constant is defined as

$$T_L = Lf_s / R \quad (11)$$

Where is switching frequency

$$f_s = 1/T_s \quad (12)$$

The voltage in DCM is

$$M_{DCM} = V_o/V_{in} = 1/2 + \sqrt{\frac{1}{4} + \frac{D2}{TL}} \quad (13)$$

III. Boundary Operating Condition between CCM and DCM

If the proposed converter I is operated in boundary conduction mode (BCM), the voltage gain of the CCM operation is equal to the voltage gain of the DCM operation. From (4) and (12), the boundary normalized inductor time constant T_{LB} can be derived as follows:

$$T_{LB} = D(1-D)^2/2(1+D) \quad (14)$$

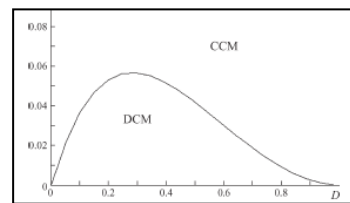


Fig: 5

The curve T_{LB} is shown in Fig 5. If T_L is greater than T_{LB}, the proposed converter I is operated in CCM. If T_L is lesser than T_{LB}, the proposed converter I is operated in DCM.

C. Converter –II

A capacitor is added in series with the load of converter- I such that it charges in mode:1 which adds up the output voltage the arrangement is shown in Fig: 6.

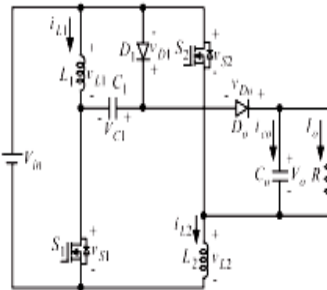


Fig: 6

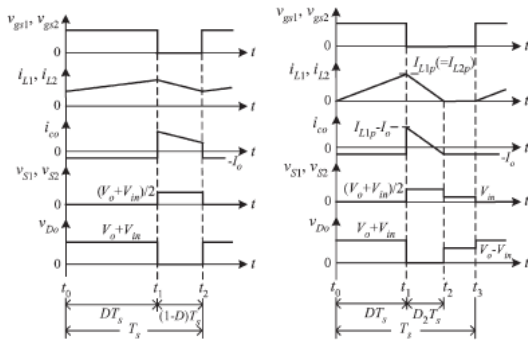


Fig: 7

Switches S1 and S2 are controlled simultaneously by one control signal. Thus, two inductors L1 and L2 with the same level of inductance are also adopted in this converter. Some typical waveforms of CCM and DCM are shown 7. The operating principle and steady state analysis is shown by taking different modes in CCM and DCM.

I. CCM Operation

The operating principle of Converter –II can be divided into two modes

1. Modes [t₀, t₁]: During this interval S₁ and S₂ are switched on as shown in Fig. 8(a). The inductors L₁ and L₂ are charged in parallel from dc source and which are having equal capacity of inductance, and the energy stored in C_o is released to the load. Moreover, capacitor C₁ is charged from the dc source.

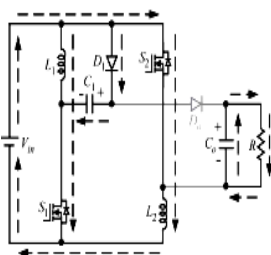


Fig: 8 (a)

Thus, the voltages across L₁, L₂, and C₁ are given as

$$V_{L1} = V_{L2} = V_{C1} = V_{in} \tag{15}$$

2. Mode [t₁, t₂]: During this time interval, S₁ and S₂ are turned off. The equivalent circuit is shown in Fig. 8(b). The dc source, L₁, C₁, and L₂ are series connected to transfer the energies to C_o and the load. Thus, the voltages across L₁ and L₂ are derived as

$$V_{L1} = V_{L2} = \frac{V_{in} + V_{c1} - V_0}{2} = \frac{2V_{in} - V_0}{2} \tag{16}$$

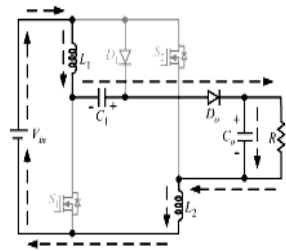


Fig: 8 (b)

By using the volt–second balance principle on L₁ and L₂, the following can be obtained:

$$\int_0^{DT_s} V_{in} dt + \int_{DT_s}^{T_s} \frac{2V_{in} - V_0}{2} dt = 0 \tag{17}$$

By simplifying (16), the voltage gain is given by

$$M_{CCM} = \frac{V_o}{V_{in}} = \frac{2}{1 - D} \tag{18}$$

From Fig. 8(a), the voltage stresses on S₁, S₂, D₁, and D_o are derived as

$$\left. \begin{aligned} V_{S1} = V_{S2} = V_{D1} = V_0/2 \\ V_{D0} = V_0 \end{aligned} \right\} \tag{19}$$

Explaining research chronological, including research design, research procedure (in the form of algorithms, Pseudocode or other), how to test and data acquisition [1]-[3]. The description of the course of research should be supported references, so the explanation can be accepted scientifically [2], [4].

II DCM Operation

The operating modes can be divided into three modes, defined as 1, 2 and 3.

1. Mode 1 [t₀, t₁]: The operating principle is the same as that for mode 1 of the CCM operation. The two peak currents of L₁ and L₂ can be found as

$$I_{L1p} = I_{L2p} = V_{in}DT_s/L \tag{20}$$

2. Mode 2 [t₁, t₂]: During this time interval, S₁ and S₂ are turned off. The equivalent circuit is shown in Fig.8(b). The dc source, L₁, C₁, and L₂ are series connected to transfer the energies to C_o and the load. The values for i_{L1} and i_{L2} are decreased to

zero at $t = t_2$. Another expression for I_{L1p} and I_{L2p} is given as

$$I_{L1p} = I_{L2p} = \frac{V_o - V_{in} - V_{c1}}{2L} D_2 T_s = \frac{V_o - 2V_{in}}{2L} D_2 T_s \quad (21)$$

3.Mode 3 [t_2, t_3] :During this time interval, S_1 and S_2 are still turned off.the equivalent circuit is shown in Fig 8(c).

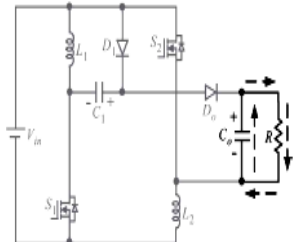


Fig: 8 (c)

The energies stored in L_1 and L_2 are zero.Thus, only the energy stored in C_o discharged to the load. From (20) and (21), D_2 is derived as follows:

$$D_2 = \frac{2DV_{in}}{V_o - 2V_{in}} \quad (22)$$

From Fig.8(b), the average output-capacitor current during each switching period is given by

$$I_{co} = \frac{\frac{1}{2}D_2T_s I_{L1p} - I_o T_s}{T_s} = \frac{1}{2}D_2 I_{L1p} - I_o \quad (23)$$

By substituting (21) and (22) into (23) , I_{co} is derived as

$$I_{co} = \frac{D^2 V_{in}^2 T_s}{L(V_o - 2V_{in})} - \frac{V_o}{R} \quad (24)$$

Since I_{co} is equal to zero under steady state, (24) can be rewritten as follows:

$$\frac{D^2 V_{in}^2 T_s}{L(V_o - 2V_{in})} = \frac{V_o}{R} \quad (25)$$

Thus, the voltage gain is given by

$$M_{DCM} = \frac{V_o}{V_{in}} = 1 + \sqrt{1 + \frac{D^2}{\tau_L}} \quad (26)$$

III. Boundary Operating Condition between CCM and DCM

If the proposed converter II is operated in BCM, the voltage gain of the CCM operation is equal to the voltage gain of the DCM operation. From (18) and (26), the boundary normalized inductor time constant τ_{LB} can be derived as

$$\tau_{LB} = \frac{D(1-D)^2}{4} \quad (27)$$

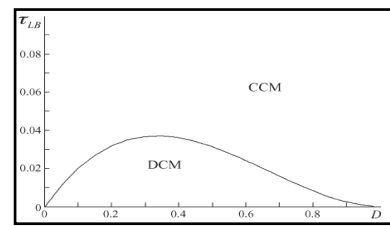


Fig:9

The curve of τ_{LB} is shown in Fig. 9. If τ_L is larger than τ_{LB} , the proposed converter II is operated in CCM.

D. Converter –III

Which is the converter I with two voltage lift circuits. Thus, two inductors (L_1 and L_2) with the same level of inductance are also adopted in this converter. Switches S_1 and S_2 are controlled simultaneously by one control signal.Fig. 10 show some typical waveforms of CCM and DCM.

The operating principles and steady-state analysis of CCM and DCM are presented as follows.

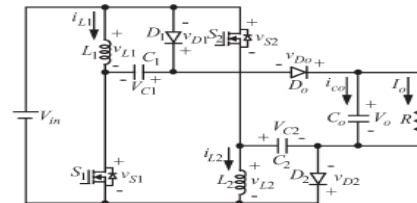


Fig:10

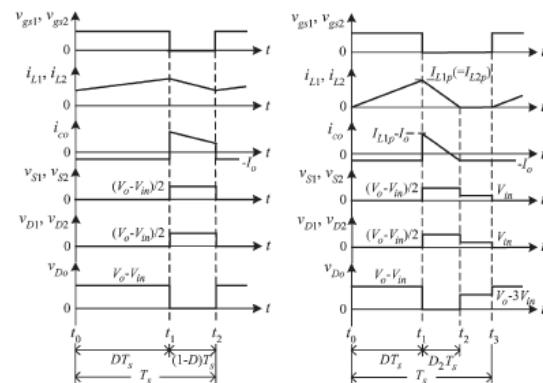


Fig: 11

I CCM Operation

The operating modes can be divided into two modes, defined as modes 1 and 2.

1) Mode 1 [t_0, t_1] : During this time interval, S_1 and S_2 are turned on. The equivalent circuit is shown in Fig. 12(a). L_1 and L_2 are charged in parallel from the dc source, and the energy stored in C_o is released to the load.

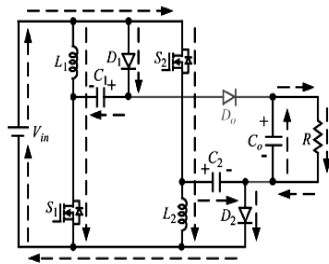


Fig: 12 (a)

Moreover, capacitors C_1 and C_2 are charged from the dc source. Thus, the voltages across L_1 , L_2 , C_1 , and C_2 are given as

$$v_{L1} = v_{L2} = V_{C1} = V_{C2} = V_{in} \quad (28)$$

2) Mode 2 [t_1, t_2]: During this time interval, S_1 and S_2 are turned off. The equivalent circuit is shown in Fig. 12(b). The dc source, L_1 , C_1 , C_2 , and L_2 are series connected to transfer the energies to C_o and the load. Thus, the voltages across L_1 and L_2 are derived as

$$v_{L1} = v_{L2} = \frac{V_{in} + V_{c1} + V_{c2} - V_o}{2} = \frac{3V_{in} - V_o}{2} \quad (29)$$

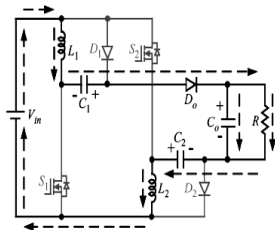


Fig: 12(b)

By using the volt-second balance principle on L_1 and L_2 , the following can be obtained:

$$\int_0^{DT_s} V_{in} dt + \int_{DT_s}^{T_s} \frac{3V_{in} - V_o}{2} dt = 0. \quad (30)$$

By simplifying (31), the voltage gain is given by

$$M_{CCM} = \frac{V_o}{V_{in}} = \frac{3 - D}{1 - D}. \quad (31)$$

From Fig. 12(a), the voltage stresses on S_1 , S_2 , D_1 , D_2 , and D_o are derived as

$$\begin{cases} V_{S1} = V_{S2} = V_{D1} = V_{D2} = \frac{V_o - V_{in}}{2} \\ V_{D_o} = V_o - V_{in}. \end{cases} \quad (32)$$

II DCM Operation

The operating modes can be divided into three modes, defined as modes 1, 2, and 3.

1) Mode 1 [t_0, t_1]: The operating principle is the same as that for mode 1 of CCM operation. The two peak currents of L_1 and L_2 can be found as

$$I_{L1p} = I_{L2p} = \frac{V_{in} DT_s}{L} \quad (33)$$

2) Mode 2 [t_1, t_2]: During this time interval, S_1 and S_2 are turned off. The equivalent circuit is shown in Fig. 12(b). The dc source, L_1 , C_1 , C_2 , and L_2 are series connected to transfer the energies to C_o and the load. The values for i_{L1} and i_{L2} are decreased to zero at $t = t_2$. Another expression for I_{L1p} and I_{L2p} is given as

$$\begin{aligned} I_{L1p} = I_{L2p} &= \frac{V_o - V_{in} - V_{c1} - V_{c2}}{2L} D_2 T_s \\ &= \frac{V_o - 3V_{in}}{2L} D_2 T_s. \end{aligned} \quad (34)$$

3) Mode 3 [t_2, t_3]: During this time interval, S_1 and S_2 are still turned off. The equivalent circuit is shown in Fig. 12(c).

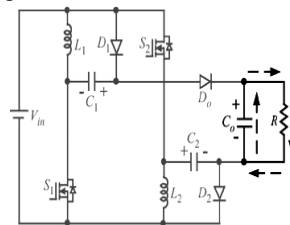


Fig: 12(c)

The energies stored in L_1 and L_2 are zero. Thus, only the energy stored in C_o is discharged to the load. From (34) and (35), D_2 is derived as follows:

$$D_2 = \frac{2DV_{in}}{V_o - 3V_{in}} \quad (35)$$

From Fig. 12(b), the average output-capacitor current during each switching period is given by

$$I_{co} = \frac{\frac{1}{2} D_2 T_s I_{L1p} - I_o T_s}{T_s} = \frac{1}{2} D_2 I_{L1p} - I_o \quad (36)$$

By substituting (34) and (36) into (37), I_{co} is derived as

$$I_{co} = \frac{D^2 V_{in}^2 T_s}{L(V_o - 3V_{in})} - \frac{V_o}{R} \quad (37)$$

Since I_{co} is equal to zero under steady state, (37) can be rewritten as follows:

$$\frac{D^2 V_{in}^2 T_s}{L(V_o - 3V_{in})} = \frac{V_o}{R} \quad (38)$$

Thus, the voltage gain is given by

$$M_{DCM} = \frac{V_o}{V_{in}} = \frac{3}{2} + \sqrt{\frac{9}{4} + \frac{D^2}{\tau_L}} \quad (39)$$

III. Boundary Operating Condition between CCM and DCM

If the proposed converter III is operated in BCM, the voltage gain of CCM operation is equal to the voltage gain of DCM operation. From

(31) and (39), the boundary normalized inductor time constant τ_{LB} can be derived as follows:

$$\tau_{LB} = \frac{D(1-D)^2}{2(3-D)} \tag{40}$$

The drawing of τ_{LB} is shown in Fig. 13. If τ_L is larger than τ_{LB} , the converter III is operated in CCM.

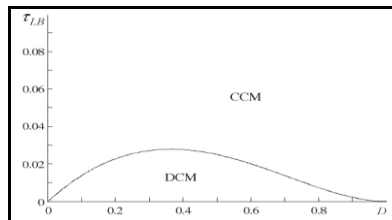


Fig: 13

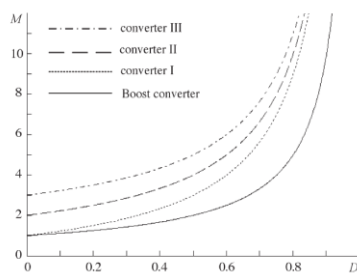


Fig: 14

Fig. 13 gives the Boundary condition of Converter – III and Fig. 14 gives the Voltage gain versus duty ratio for the boost Converter and the three proposed converters.

E. Comparison of Proposed Converters and Boost Converters

The voltage stresses on the active switch and the voltage gains of the boost converter and the proposed converters are summarized in Table I.

	M_{CCM}	Voltage stress
Boost Converter	$1/(1-D)$	V_o
Converter – I	$(1+D)/(1-D)$	$(V_o+V_{in})/2$
Converter – II	$2/(1-D)$	$V_o/2$
Converter – III	$(3-D)/(1-D)$	$(V_o-V_{in})/2$

TABLE – I

The voltage stresses on the active switch of the three proposed converters are less than the voltage stress on the active switch of the boost converter, and thus, the active switches with low voltage ratings and low ON-state resistance levels $RDS_{(ON)}$ can be selected. Moreover, the curves of the voltage gain of the boost converter and the proposed converters are shown in Fig. 12. As illustrated, the proposed converters can achieve high step-up voltage gain.

3. PHOTO VOLTAIC SYSTEM:

It is well known that renewable energy sources are attractive options for providing power in places where a connection to the utility network is either impossible or unduly expensive. Photovoltaic (PV) generation systems and isolated wind-electric systems are considered among the renewable systems to be viable alternatives for the designer of such remote power supplies. Nevertheless, systems based on either wind or solar energy is unreliable due to seasonal and diurnal variations of these resources. Earlier, wind-diesel systems were employed to overcome the diluteness of the renewable resources, but the recurring need of the diesel oil and frequent maintenance requirement of the diesel-generators made such a system to be inappropriate for off-grid supplies. The control of such a scheme is also far from straightforward, especially where there is a high wind penetration. Furthermore, it decreases the advantage of clean and nonpolluting energy achieved from the renewable sources. Photovoltaic (PV) generation is gaining increased importance as a renewable source due to its advantages like absence of fuel cost, little maintenance, no noise and wear due to absence of Moving parts.

4. Proposed Converter System for photo voltaic system

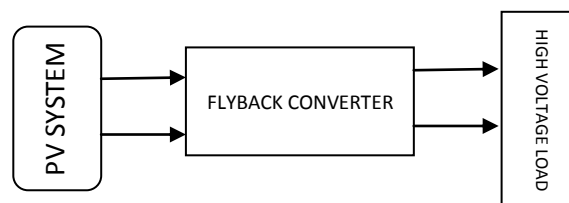


Fig: 15

Fig: 15 gives the block diagram representation of proposed Flyback converter fed with photovoltaic system for high voltages. From the figure it is evident that the voltage generated by photo voltaic system is fed to Flyback Converters (I, II, III) after filtering the voltage. Then the converters operate as mentioned in section 2 by which required high voltage DC is obtained.

5. RESULTS AND DISCUSSIONS

A. For Converter-I

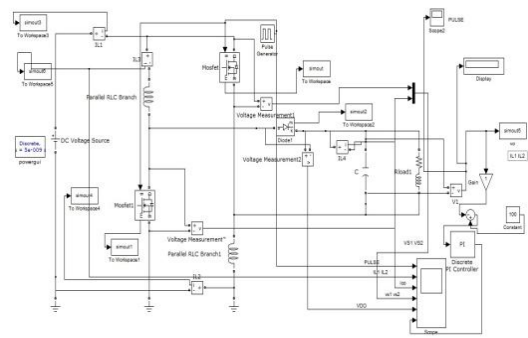


Fig: 16

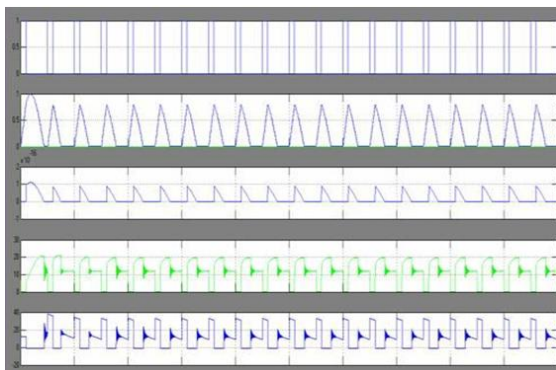


Fig: 17

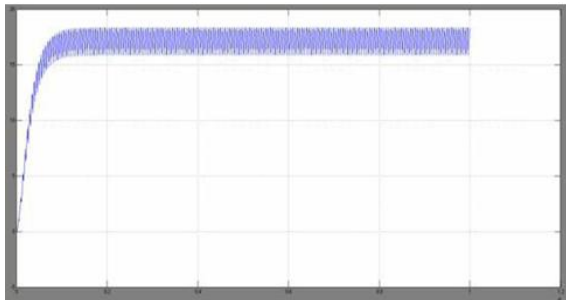


Fig:18

Fig:16 gives the matlab simlink model of Converter – I implemented in CCM and DCM Modes. Fig: 17 gives gate pulse, Inductive current, Capacitive current, Voltages across the switches S1 and S₂. Fig: 18 gives the output voltage of Converter –I connected to a photo voltaic system of 12V, for which the output voltage is observed as 22V for 0.2 duty ratio.

B. For Converter-II

Fig:19 gives the matlab simlink model of Converter – II implemented in CCM and DCM Modes. Fig: 20 gives gate pulse, Inductive current, Capacitive current, Voltages across the switches S1 and S₂,

Diode Current. Fig: 21 gives the output voltage of Converter –II connected to a photo voltaic system of 12V, for which the output voltage is observed as 26V for 0.2 duty ratio.

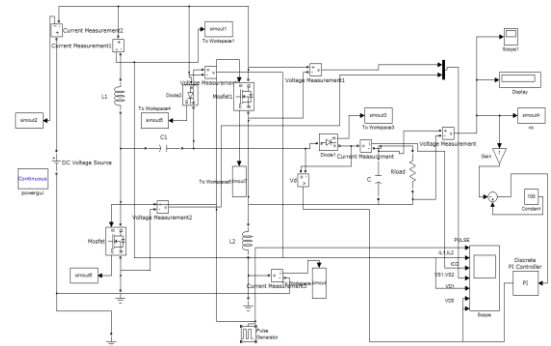


Fig: 19

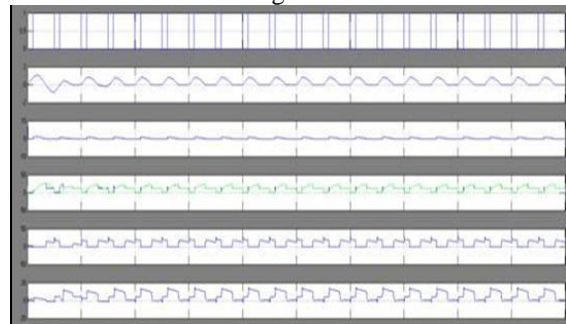


Fig: 20

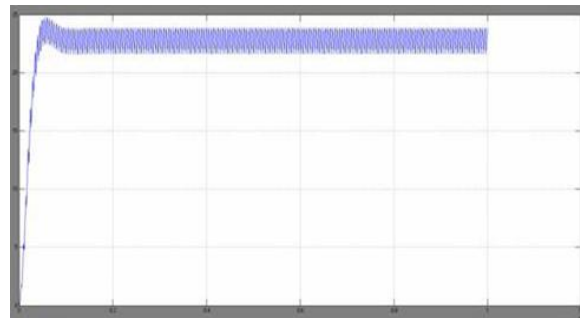


Fig: 21

C. For Converter-III

Fig: 22 gives the matlab simlink model of Converter – III implemented in CCM and DCM Modes. Fig: 23 gives gate pulse, Inductive currents, Voltages across the switches S1 and S₂. Fig: 24 give the output voltage of Converter –III connected to a photo voltaic system of 12V, for which the output voltage is observed as 28V for 0.2 duty ratio.

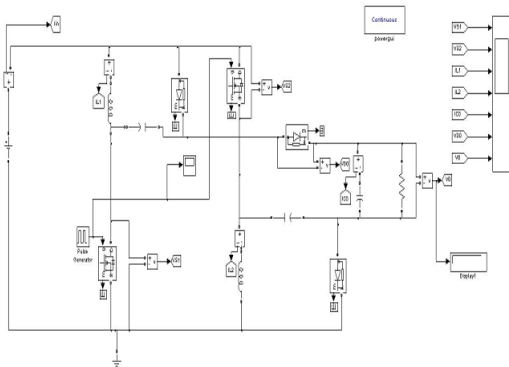


Fig: 22

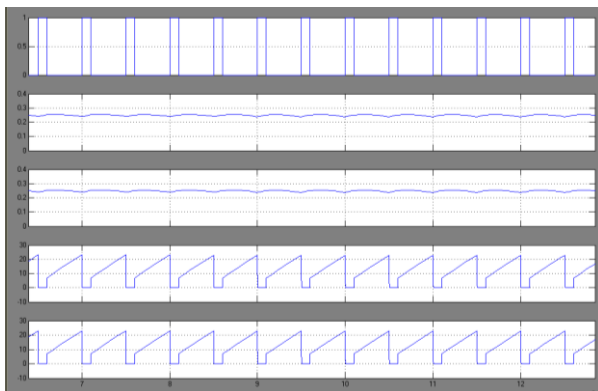


Fig: 23

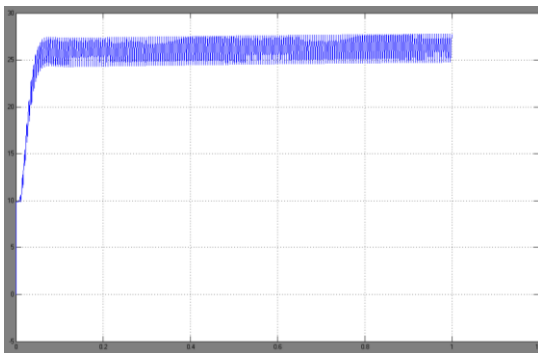


Fig: 24

Duty Ratio	Output Voltage (V)
30	32
40	38
50	45
60	56
70	75
80	105
90	123

TABLE – II

Table – II gives the information about the output voltages of converter – III for different duty ratios,

from which it is clear that higher voltage gains can be achieved with less voltage stress on the switches.

5. Conclusions

Solar energy is rapidly growing alternative renewable energy source for which the high voltage gain fly back converters are proposed. The structures of the converters are very simple. Since the voltage stresses on the active switches are low, active switches with low voltage ratings and low ON-state resistance levels $R_{DS(ON)}$ can be selected. The steady-state analyses of the voltage gain and the boundary operating condition are discussed in detail. The proposed system is feasible for operating high voltage loads by 12V photovoltaic system with the help of three fly back converters.

References

- [1] B. Bryant and M. K. Kazimierczuk, “Voltage-loop power-stage transfer functions with MOSFET delay for boost PWM converter operating in CCM,” IEEE Trans. Ind. Electron., vol. 54, no. 1, pp. 347–353, Feb. 2007.
- [2] X. Wu, J. Zhang, X. Ye, and Z. Qian, “Analysis and derivations for a family ZVS converter based on a new active clamp ZVS cell,” IEEE Trans. Ind. Electron., vol. 55, no. 2, pp. 773–781, Feb. 2008.
- [3] C. Lu, K. W. Cheng, and Y. S. Lee, “A single-switch continuous conduction-mode boost converter with reduced reverse-recovery and switching losses,” IEEE Trans. Ind. Electron., vol. 50, no. 4, pp. 767–776, Aug. 2003.
- [4] N. P. Papanikolaou and E. C. Tatakis, “Active voltage clamp in fly back converters operating in CCM mode under wide load variation,” IEEE Trans. Ind. Electron., vol. 51, no. 3, pp. 632–640, Jun. 2004.
- [5] B. R. Lin and F. Y. Hsieh, “Soft-switching zeta-flyback converter with a buck-boost type of active clamp,” IEEE Trans. Ind. Electron., vol. 54, no. 5, pp. 2813–2822, Oct. 2007.
- [6] C. M. Wang, “A novel ZCS-PWM flyback converter with a simple ZCSPWM commutation cell,” IEEE Trans. Ind. Electron., vol. 55, no. 2, pp. 749–757, Feb. 2008.
- [7] T. F. Wu, Y. S. Lai, J. C. Hung, and Y. M. Chen, “Boost converter with coupled inductors and buck-boost type of active clamp,” IEEE Trans. Ind. Electron., vol. 55, no. 1, pp. 154–162, Jan. 2008.
- [8] K. C. Tseng and T. J. Liang, “Novel high-efficiency step-up converter,” Proc. Inst. Elect. Eng.—Elect. Power Appl., vol. 151, no. 2, pp. 182–190, Mar. 2004. IEEE TRANSACTIONS ON INDUSTRIAL ELECTRONICS, VOL. 56, NO. 8, AUGUST 2009
- [9] R. J. Wai, C. Y. Lin, R. Y. Duan, and Y. R. Chang, “High-efficiency DC–DC converter with high voltage gain and reduced switch stress,” IEEE Trans. Ind. Electron., vol. 54, no. 1, pp. 354–364, Feb. 2007.
- [10] R. J. Wai, C. Y. Lin, C. Y. Lin, R. Y. Duan, and Y. R. Chang, “High efficiency power conversion system for kilowatt-level stand-alone generation unit with low input voltage,” IEEE Trans. Ind. Electron., vol. 55, no. 10, pp. 3702–3714, Oct. 2008.

- [11] J. W. Baek, M. H. Ryoo, T. J. Kim, D. W. Yoo, and J. S. Kim, "High boost converter using voltage multiplier," in Proc. IEEE IECON, 2005, pp. 567–572.
- [12] Q. Zhao and F. C. Lee, "High-efficiency, high step-up DC–DC converters," IEEE Trans. Power Electron., vol. 18, no. 1, pp. 65–73, Jan. 2003.
- [13] R. J. Wai and R. Y. Duan, "High-efficiency DC/DC converter with high voltage gain," Proc. Inst. Elect. Eng.—Elect. Power Appl., vol. 152, no. 4, pp. 793–802, Jul. 2005.
- [14] G. A. L. Henn, L. H. S. C. Barreto, D. S. Oliveira, Jr., and E. A. S. Silva, "A novel bidirectional interleaved boost converter with high voltage gain," in Proc. IEEE APEC, 2008, pp. 1589–1594.
- [15] G. V. T. Bascope, R. P. T. Bascope, D. S. Oliveira, Jr., S. A. Vasconcelos, F. L. M. Antunes, and C. G. C. Branco, "A high step-up DC–DC converter based on three-state switching cell," in Proc. IEEE ISIE, 2006, pp. 998–1003.
- [16] L. Huber and M. M. Jovanovic, "A design approach for server power supplies for networking applications," in Proc. IEEE APEC, 2000, pp. 1163–1169.
- [17] L. H. Barreto, E. A. Coelho, V. J. Farias, J. C. Oliveira, L. C. Freitas, and J. B. Vieira, "A quasi-resonant quadratic boost converter using a single resonant network," IEEE Trans. Ind. Electron., vol. 52, no. 2, pp. 552–557, Apr. 2005.
- [18] L. Luo and H. Ye, "Positive output multiple-lift push-pull switched-capacitor Luo-converters," IEEE Trans. Ind. Electron., vol. 51, no. 3, pp. 594–602, Jun. 2004.
- [19] L. Luo, "Six self-lift DC–DC converters, voltage lift technique," IEEE Trans. Ind. Electron., vol. 48, no. 6, pp. 1268–1272, Dec. 2001.
- [20] R. Gules, L. L. Pfiftscher, and L. C. Franco, "An interleaved boost DC–DC converter with large conversion ratio," in Proc. IEEE ISIE, 2003, pp. 411–416. [21] D. Zhou, A. Pietkiewicz, and S. Cuk, "A three-switch high-voltage converter," IEEE Trans. Power Electron., vol. 14, no. 1, pp. 177–183, Jan. 1999.
- [21] D. Zhou, A. Pietkiewicz, and S. Cuk, "A three-switch high-voltage converter," IEEE Trans. Power Electron., vol. 14, no. 1, pp. 177–183, Jan. 1999.
- [22] B. Axelrod, Y. Berkovich, and A. Ioinovici, "Transformerless DC–DC converters with a very high DC line-to-load voltage ratio," in Proc. IEEE ISCAS, 2003, pp. III-435–III-438.
- [23] O. Abutbul, A. Gherlitz, Y. Berkovich, and A. Ioinovici, "Step-up switching-mode converter with high voltage gain using a switched capacitor circuit," IEEE Trans. Circuits Syst. I, Fundam. Theory Appl., vol. 50, no. 8, pp. 1098–1102, Aug. 2003.
- [24] B. Axelrod, Y. Berkovich, and A. Ioinovici, "Switched-capacitor/switched-inductor structures for getting transformerless hybrid DC–DC PWM converters," IEEE Trans. Circuits Syst. I, Reg. Papers, vol. 55, no. 2, pp. 687–696, Mar. 2008.

ABOUT THE AUTHORS.



J V Pavan Chand was born in India and received his B.Tech Degree in Electrical and Electronics engineering from Jawaharlal Nehru Technological University Hyderabad, presently he is pursuing his master degree in **Sri Vasavi Engineering College** affiliated to JNTUK, Kakinada. His area of Specialization is Power Electronics



Nandigam Sri Harish was born in India and received his Master Degree with specialization of Power System-High Voltage Engineering in Jawaharlal Nehru Technological University, Kakinada and received his B.E in Electrical and Electronics Engineering from Anna University. Presently he is working as assistant Professor in Sri Vasavi Engineering College. His Area of interest is Power Electronics and power system.



Chunduri Rambabu was born in India and received his Master Degree in Jawaharlal Nehru Technological University, Anantapur and received his B.Tech in Electrical and Electronics Engineering from University of Madras. Presently he is working as Professor and HOD in Sri Vasavi Engineering College. His Area of interest is Power Electronics and power system.

V. Sravan Kumar was born in India and received his Master Degree with specialization of Power Electronics in National Institute of technology, Tiruchy and received his B.Tech in Electrical and Electronics Engineering from Jawaharlal Nehru Technological University Hyderabad. Presently he is working as assistant Professor in Lakireddy Bali Reddy College Of Engineering. His Area of interest is Power Electronics and Drives.